# Erratum: Dynamical coupled-channels model of $K^- p$ reactions. II. Extraction of $\Lambda^*$ and $\Sigma^*$ hyperon resonances [Phys. Rev. C 92, 025205 (2015)]

H. Kamano, S. X. Nakamura, T.-S. H. Lee, and T. Sato

(Received 25 March 2017; published 12 April 2017)

DOI: 10.1103/PhysRevC.95.049903

There were some typographical errors in the numerical values listed in Tables II, IV, and VII of the original paper. They are corrected in this Erratum where the corrections are emphasized with bold font. Also, in Fig. 8 of the original paper, the blue diamond pointing out the position of pole B1 on the complex-$W$ plane was misplaced, and the corrected figure is presented here.

TABLE II. Extracted complex pole masses ($M_R$) for the $\Lambda^*$ and $\Sigma^*$ resonances found in the energy region above the $\bar{K}N$ threshold. The masses are listed as [Re($M_R$), $-$ Im($M_R$)] together with their deduced uncertainties. The resonance poles are searched in the complex-$W$ region with $m_{\bar{K}} + m_N \leqslant \mathrm{Re}(W) \leqslant 2.1$ and $0 \leqslant -\mathrm{Im}(W) \leqslant 0.2$ GeV, and all of the resonances listed are located in the complex-$W$ Riemann surface nearest to the physical real $W$ axis.

| | $J^P(l_{I2J})$ | $M_R$ (MeV) | |
|---|---|---|---|
| | | Model A | Model B |
| $\Lambda$ baryons | $1/2^-(S_{01})$ | $(1669^{+3}_{-8}, 9^{+9}_{-1})$ | $(1512^{+1}_{-1}, 185^{+1}_{-2})$ |
| | | | $(1667^{+1}_{-2}, 12^{+3}_{-1})$ |
| | $1/2^+(P_{01})$ | $(1544^{+3}_{-3}, 56^{+6}_{-1})$ | $(\mathbf{1547}^{+5}_{-6}, 82^{+7}_{-7})$ |
| | | $(2097^{+40}_{-1}, 83^{+32}_{-6})$ | $(1841^{+3}_{-4}, 31^{+3}_{-2})$ |
| | $3/2^+(P_{03})$ | $(1859^{+5}_{-7}, 56^{+10}_{-2})$ | $(1671^{+2}_{-8}, 5^{+11}_{-2})$ |
| | $3/2^-(D_{03})$ | $(1517^{+4}_{-4}, 8^{+5}_{-4})$ | $(1517^{+4}_{-3}, 8^{+6}_{-6})$ |
| | | $(1697^{+6}_{-6}, 33^{+7}_{-7})$ | $(1697^{+6}_{-5}, 37^{+7}_{-7})$ |
| | $5/2^-(D_{05})$ | $(1766^{+37}_{-34}, 106^{+47}_{-31})$ | $(1924^{+52}_{-24}, 45^{+57}_{-17})$ |
| | | $(1899^{+35}_{-37}, 40^{+50}_{-17})$ | |
| | $5/2^+(F_{05})$ | $(1824^{+2}_{-1}, 39^{+1}_{-1})$ | $(1821^{+1}_{-1}, 32^{+1}_{-1})$ |
| | $7/2^+(F_{07})$ | (1757,73) | $(2041^{+80}_{-82}, 119^{\mathbf{+86}}_{\mathbf{-70}})$ |
| $\Sigma$ baryons | $1/2^-(S_{11})$ | $(1704^{+3}_{-6}, 43^{+7}_{-2})$ | $(1551^{+2}_{-9}, 188^{+6}_{-1})$ |
| | | | $(1940^{+2}_{-2}, 86^{+2}_{-2})$ |
| | $1/2^+(P_{11})$ | $(1547^{+111}_{-59}, 92^{+43}_{-39})$ | $(1457^{+5}_{-1}, 39^{+1}_{-4})$ |
| | | $(1706^{+67}_{-60}, 51^{+79}_{-42})$ | $(1605^{+2}_{-4}, 96^{+1}_{-5})$ |
| | | | $(2014^{+6}_{-13}, 70^{+14}_{-1})$ |
| | $3/2^-(D_{13})$ | $(1607^{+13}_{-11}, 126^{+15}_{-9})$ | $(1492^{+4}_{-7}, 69^{+4}_{-7})$ |
| | | $(1669^{+7}_{-7}, 32^{+5}_{-7})$ | $(1672^{+5}_{-10}, 33^{+3}_{-3})$ |
| | $5/2^-(D_{15})$ | $(1767^{+2}_{-2}, 64^{+2}_{-1})$ | $(1765^{+2}_{-1}, 64^{+3}_{-1})$ |
| | $5/2^+(F_{15})$ | $(1890^{+3}_{-2}, 49^{+2}_{-3})$ | $(1695^{+20}_{-77}, 97^{+50}_{-44})$ |
| | $7/2^+(F_{17})$ | $(2025^{+10}_{-5}, 65^{+3}_{-12})$ | $(2014^{+12}_{-1}, 103^{+3}_{-9})$ |

 

TABLE IV. Residues $R_{MB,\bar{K}N}$ for the unstable channels $MB = \pi\Sigma^*, \bar{K}^*N$. The values presented are of the resonances extracted from Model A. The magnitude [$R$ (MeV)] and phase [$\phi$ (degree), taken to be $-180^\circ < \phi \leqslant 180^\circ$] of $R_{MB,\bar{K}N} \equiv \mathrm{Re}^{i\phi}$ are listed. Each resonance is specified by the real part of the pole mass $\mathrm{Re}(M_R)$ and its quantum numbers. The quantum numbers for the $(\pi\Sigma^*)_i$ $(i = 1,2)$ and $(\bar{K}^*N)_i$ $(i = 1$–$3)$ channels for a given $J^P$ are presented in Table I.

| Particle $J^P(l_{I2J})$ | $R_{(\pi\Sigma^*)_1,\bar{K}N}$ | | $R_{(\pi\Sigma^*)_2,\bar{K}N}$ | | $R_{(\bar{K}^*N)_1,\bar{K}N}$ | | $R_{(\bar{K}^*N)_2,\bar{K}N}$ | | $R_{(\bar{K}^*N)_3,\bar{K}N}$ | |
|---|---|---|---|---|---|---|---|---|---|---|
| | $R$ | $\phi$ | $R$ | $\phi$ | $R$ | $\phi$ | $R$ | $\phi$ | $R$ | $\phi$ |
| $\Lambda(1669)1/2^-(S_{01})$ | 0.94 | −104 | | | | | | | | |
| $\Lambda(1544)1/2^+(P_{01})$ | 10.21 | 77 | | | | | | | | |
| $\Lambda(2097)1/2^+(P_{01})$ | 20.32 | **−10** | | | 13.24 | −97 | 4.14 | 2 | | |
| $\Lambda(1859)3/2^+(P_{03})$ | 16.65 | −40 | 3.61 | 127 | 10.63 | −160 | 11.80 | 15 | 0.79 | 129 |
| $\Lambda(1517)3/2^-(D_{03})$ | 3.29 | −123 | 0.11 | 122 | | | | | | |
| $\Lambda(1697)3/2^-(D_{03})$ | 4.37 | 168 | 10.42 | −22 | | | | | | |
| $\Lambda(1766)5/2^-(D_{05})$ | 8.50 | 87 | 0.43 | −109 | | | | | | |
| $\Lambda(1899)5/2^-(D_{05})$ | 0.95 | 113 | 0.03 | 127 | 1.11 | −177 | 1.02 | 3 | 0.31 | −17 |
| $\Lambda(1824)5/2^+(F_{05})$ | 13.11 | 161 | 7.75 | 151 | 0.29 | 41 | 6.58 | −139 | 0.02 | 161 |
| $\Lambda(1757)7/2^+(F_{07})$ | 0.33 | −82 | 0.002 | −128 | | | | | | |
| Particle $J^P(l_{I2J})$ | $R_{(\pi\Sigma^*)_1,\bar{K}N}$ | | $R_{(\pi\Sigma^*)_2,\bar{K}N}$ | | $R_{(\bar{K}^*N)_1,\bar{K}N}$ | | $R_{(\bar{K}^*N)_2,\bar{K}N}$ | | $R_{(\bar{K}^*N)_3,\bar{K}N}$ | |
| | $R$ | $\phi$ | $R$ | $\phi$ | $R$ | $\phi$ | $R$ | $\phi$ | $R$ | $\phi$ |
| $\Sigma(1704)1/2^-(S_{11})$ | 2.31 | 73 | | | | | | | | |
| $\Sigma(1547)1/2^+(P_{11})$ | 4.71 | −44 | | | | | | | | |
| $\Sigma(1706)1/2^+(P_{11})$ | 3.65 | −128 | | | | | | | | |
| $\Sigma(1607)3/2^-(D_{13})$ | 4.65 | −18 | 1.31 | 123 | | | | | | |
| $\Sigma(1669)3/2^-(D_{13})$ | 7.30 | 167 | 2.93 | 141 | | | | | | |
| $\Sigma(1767)5/2^-(D_{15})$ | 25.05 | 137 | 0.83 | −58 | | | | | | |
| $\Sigma(1890)5/2^+(F_{15})$ | 3.51 | 161 | 0.79 | −163 | 0.23 | 4 | 2.40 | 51 | 0.02 | 16 |
| $\Sigma(2025)7/2^+(F_{17})$ | 5.78 | −23 | 1.59 | 132 | 12.54 | 38 | 20.76 | 37 | 0.23 | 22 |

TABLE VII. Branching ratios for the decays of $\Lambda^*$ and $\Sigma^*$ resonances extracted from Model A. Equations (23)–(26) are used for evaluating the ratios. The quantum numbers for the $(\pi\Sigma^*)_i$ $(i = 1,2)$ and $(\bar{K}^*N)_i$ $(i = 1$–$3)$ channels for a given $J^P$ are presented in Table I.

| Particle $J^P(l_{I2J})$ | Branching ratios (%) | | | | | | | | |
|---|---|---|---|---|---|---|---|---|---|
| | $B_{\bar{K}N}$ | $B_{\pi\Sigma}$ | $B_{\eta\Lambda}$ | $B_{K\Xi}$ | $B_{(\pi\Sigma^*)_1}$ | $B_{(\pi\Sigma^*)_2}$ | $B_{(\bar{K}^*N)_1}$ | $B_{(\bar{K}^*N)_2}$ | $B_{(\bar{K}^*N)_3}$ |
| $\Lambda(1669)1/2^-(S_{01})$ | 31.8 | 28.9 | 37.3 | | 1.9 | | 0.0 | 0.0 | |
| $\Lambda(1544)1/2^+(P_{01})$ | 6.4 | 85.1 | | | 8.5 | | | | |
| $\Lambda(2097)1/2^+(P_{01})$ | 22.5 | 0.9 | 11.1 | 5.1 | 47.0 | | **13.0** | **0.3** | |
| $\Lambda(1859)3/2^+(P_{03})$ | 30.5 | 4.0 | 1.2 | 0.9 | 45.3 | 1.9 | 7.3 | 8.8 | 0.1 |
| $\Lambda(1517)3/2^-(D_{03})$ | 43.0 | 44.6 | | | 12.1 | 0.3 | | | |
| $\Lambda(1697)3/2^-(D_{03})$ | 23.9 | 38.7 | 0.0 | | 6.2 | 30.8 | 0.0 | 0.3 | 0.0 |
| $\Lambda(1766)5/2^-(D_{05})$ | 4.6 | 62.1 | 0.7 | | 32.4 | 0.1 | 0.1 | 0.1 | 0.0 |
| $\Lambda(1899)5/2^-(D_{05})$ | 0.6 | 1.7 | 2.4 | 56.2 | 13.4 | 0.0 | 13.4 | 11.5 | 0.9 |
| $\Lambda(1824)5/2^+(F_{05})$ | 54.7 | 21.8 | 0.1 | 0.0 | 17.3 | 5.5 | 0.0 | 0.6 | 0.0 |
| $\Lambda(1757)7/2^+(F_{07})$ | 0.0 | 89.1 | 0.2 | | 10.5 | 0.0 | 0.0 | 0.1 | 0.0 |
| Particle $J^P(l_{I2J})$ | $B_{\bar{K}N}$ | $B_{\pi\Sigma}$ | $B_{\pi\Lambda}$ | $B_{K\Xi}$ | $B_{(\pi\Sigma^*)_1}$ | $B_{(\pi\Sigma^*)_2}$ | $B_{(\bar{K}^*N)_1}$ | $B_{(\bar{K}^*N)_2}$ | $B_{(\bar{K}^*N)_3}$ |
| $\Sigma(1704)1/2^-(S_{11})$ | 15.4 | 37.3 | 43.5 | | 2.4 | | 0.4 | 1.0 | |
| $\Sigma(1547)1/2^+(P_{11})$ | 0.5 | 86.5 | 12.8 | | 0.1 | | | | |
| $\Sigma(1706)1/2^+(P_{11})$ | 1.6 | 59.5 | 28.3 | | 10.3 | | 0.4 | 0.0 | |
| $\Sigma(1607)3/2^-(D_{13})$ | 0.3 | 38.7 | 49.0 | | 12.0 | 0.1 | 0.0 | 0.0 | 0.0 |
| $\Sigma(1669)3/2^-(D_{13})$ | 12.1 | 46.5 | 5.8 | | 30.9 | 4.4 | 0.1 | 0.2 | 0.1 |
| $\Sigma(1767)5/2^-(D_{15})$ | 40.2 | 4.2 | 24.4 | | 30.9 | 0.0 | 0.0 | 0.3 | 0.0 |
| $\Sigma(1890)5/2^+(F_{15})$ | 3.6 | 67.8 | 12.7 | 0.0 | 11.2 | 0.4 | 0.1 | 4.2 | 0.0 |
| $\Sigma(2025)7/2^+(F_{17})$ | 26.9 | 3.7 | 8.0 | 0.6 | 3.0 | 0.3 | 15.4 | 42.2 | 0.0 |

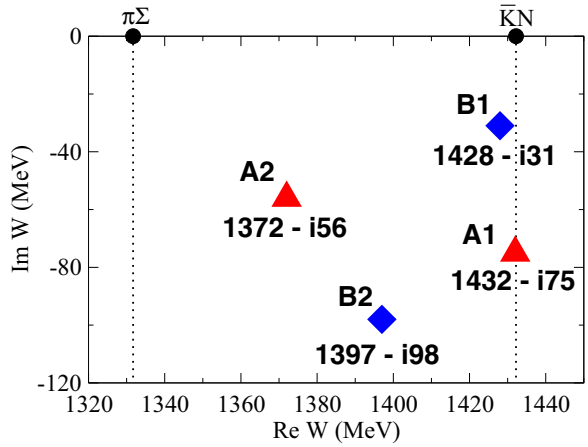


FIG. 8. $S$-wave ($J^P = 1/2^-$) $\Lambda$ resonances in the $\bar{K}N$ subthreshold region. The red triangles (blue diamonds) are resonance poles found from Model A (Model B).